5098–5108 *Nucleic Acids Research, 2011, Vol. 39, No. 12* *Published online 11 March 2011*
doi:10.1093/nar/gkr052

Actin and myosin contribute to mammalian mitochondrial DNA maintenance

A. Reyes[1], J. He[1], C. C. Mao[1], L. J. Bailey[1], M. Di Re[1], H. Sembongi[1], L. Kazak[1], K. Dzionek[1], J. B. Holmes[1,2], T. J. Cluett[1], M. E. Harbour[3], I. M. Fearnley[1], R. J. Crouch[2], M. A. Conti[4], R. S. Adelstein[4], J. E. Walker[1] and I. J. Holt[1,*]

[1]MRC Mitochondrial Biology Unit, Cambridge, UK, [2]Program in Genomics of Differentiation, Eunice Kennedy Shriver National Institute of Health and Human Development, National Institutes of Health, Bethesda, MD 20892, USA, [3]Cambridge Institute for Medical Research, Cambridge, UK and [4]Laboratory of Molecular Cardiology, National Heart, Lung and Blood Institute, NIH Bethesda, MD, USA

Received August 23, 2010; Revised January 18, 2011; Accepted January 19, 2011

ABSTRACT

Mitochondrial DNA maintenance and segregation are dependent on the actin cytoskeleton in budding yeast. We found two cytoskeletal proteins among six proteins tightly associated with rat liver mitochondrial DNA: non-muscle myosin heavy chain IIA and β-actin. In human cells, transient gene silencing of *MYH9* (encoding non-muscle myosin heavy chain IIA), or the closely related *MYH10* gene (encoding non-muscle myosin heavy chain IIB), altered the topology and increased the copy number of mitochondrial DNA; and the latter effect was enhanced when both genes were targeted simultaneously. In contrast, genetic ablation of non-muscle myosin IIB was associated with a 60% decrease in mitochondrial DNA copy number in mouse embryonic fibroblasts, compared to control cells. Gene silencing of β-*actin* also affected mitochondrial DNA copy number and organization. Protease-protection experiments and iodixanol gradient analysis suggest some β-actin and non-muscle myosin heavy chain IIA reside within human mitochondria and confirm that they are associated with mitochondrial DNA. Collectively, these results strongly implicate the actomyosin cytoskeleton in mammalian mitochondrial DNA maintenance.

INTRODUCTION

A complex protein apparatus is required to ensure the maintenance, reproduction and transmission of mitochondrial DNA (mtDNA) (1–3). In budding yeast the actin cytoskeleton plays important roles in the transmission of mitochondria and mtDNA to daughter cells (1). In mammals, studies of axonal mitochondrial transport have linked kinesin motors and microtubule filaments to the rapid transport of mitochondria over long distances, whereas mitochondrial movement over short distances is dependent on an actin-based motor (4). Hollenbeck and Saxton also suggest that members of the myosin families I, II, V and VI could act as molecular motors for mitochondrial movement along actin cables. However, the only family member shown to be associated with mitochondria hitherto is Myo19 (5).

Mitochondrial DNA segregation and transmission in budding yeast is an actin-dependent process (6). Mammalian mtDNA maintains strong contacts with the cytoskeleton (7), yet the specific proteins involved have not been defined. There have been hints that β-actin might be linked to mammalian mtDNA, it was immunoprecipitated by an antibody to the mtDNA binding protein TFAM (8), it co-purified with tagged MTERF2 (9) and β-actin was among proteins co-sedimenting with a fraction of mtDNA from HeLa cells (10). However, β-actin is a highly abundant cellular protein and a frequent contaminant in protein purification experiments suggesting that these results should be treated with caution. Indeed Pellegrini *et al*. (2009) quite reasonably assumed β-actin was present as a contaminant in their MTERF2 preparations. Here we found β-actin and non-muscle myosin heavy chain IIA associated with mtDNA after stringent washing of enriched mitochondrial nucleoprotein, leading us to implement a series of biochemical and genetic tests. The results support a role for β-actin, and the actin binding proteins non-muscle myosin IIA and IIB, in mammalian mtDNA maintenance.

*To whom correspondence should be addressed. Tel: +44 12 2325 2840; Fax: +44 12 2325 2845; Email: holt@mrc-mbu.cam.ac.uk

MATERIALS AND METHODS

Isolation of mitochondrial nucleoprotein complexes

Sucrose-gradient purified rat liver mitochondria were prepared as previously (11,12). Next, 6–12 mg mitochondria were disrupted by suspension in lysis buffer: 10 mM HEPES–NaOH, pH 7.6, 0.2 mM PMSF, 1 mM EDTA, 1 mM DTT and 0.4% n-Dodecyl-β-D-maltopyranoside (DDM), at 4°C and centrifuged at 1000 g_{max} for 10 min. The supernatant (s/n 1) was re-centrifuged at 30 000g_{max} for 30 min. Next the pellet (pellet 2) was homogenized vigorously with 10 strokes every 10 min at 4°C for 2 h in 0.5 ml of 900 mM NaCl, 50 mM HEPES, 12.5 mM EDTA, 5× Complete® EDTA-free Protease Inhibitor Cocktail (Roche), 5 mM DTT. The homogenate was divided in two and centrifuged at 30 000g_{max} for 1 h. DNA was extracted from one of the final pellets (pellet 3), whereas the other was mixed with loading buffer containing 2% SDS and the proteins fractionated by PAGE; individual proteins visible after staining with Coomassie blue were digested into peptides 'in-gel' with sequencing grade trypsin (Roche), in 20 mM Tris–HCl, pH 8.0, 5 mM $CaCl_2$ overnight at 37°C. The ensuing peptide mixtures were analysed by a MALDI-TOF-TOF mass spectrometer (4700 Proteomics Analyzer, Applied Biosystems) in MS (peptide fingerprinting) and MS-MS (peptide sequencing) modes. Proteins were identified by MASCOT search with two modes: Peptide Mass Fingerprint or MS/MS data were compared with NCBInr (all entries or Rattus) protein sequence databases. Identified proteins had a Mascot score greater than a database-generated 95% confidence score for peptide mass fingerprinting data, and/or two or more peptides identified from peptide sequencing data.

Mitochondrial import assay

^{35}S-methionine labelled proteins were generated from amplified cDNAs using a TnT Quick Coupled Transcription-/Translation system™ (Promega). Labelled proteins were incubated with rat liver mitochondria purified by differential centrifugation for 120 min at 37°C (13) with the addition of supernatant from the second centrifugation step, as this was found to facilitate β-actin import into mitochondria. Products were fractionated by SDS–PAGE. Additions were 50 μg/ml trypsin, to digest protein outside mitochondria; FCCP (carbonylcyanide-p-trifluoromethoxyphenylhydrazone) to dissipate the mitochondrial membrane potential; 0.1% Triton-X100 to lyse the mitochondria.

Cell culture and siRNA

HOS and HEK cells were grown in DMEM with 10% fetal bovine serum. For short interfering RNAs (siRNA), cells growing on 6-well plates at 25–30% confluent were transfected with 5–10 nM double stranded RNA and 3 μl of Lipofectamine2000 (Invitrogen). Where indicated cells were transfected a second time, at 72 h, and examined by confocal microscopy at 144 h, or lysed for total RNA or DNA extraction. The siRNA targeting β-actin was a siLentMer validated RNA (Bio-Rad Cat # 179-0204). Double-stranded RNAs targeting, *MYH9* or *MYH10*, from iGENE (Tokyo, Japan) were as follows: *MYH9*-2806: 5′-GCGGAGAAGAAGAAGAUGCAGC AGAAG-3′, 3′-UACGCCUCUUCUUCUUCUACGUC GUC U-5′; *MYH9*-3064: 5′-AAGAACAAGCAUGAGG -CAAUGAUCAAG-3′, 3′-UAUUCUUGUUC GUACU CCGUUACUAGU-5′; *MYH10*-2783: 5′-AGUCUAGG GUUGAAGAAGAAGAAGAAG-3′, 3′-UAUCAGAU CCCAACUUCUUCUUCUUCU-5′; *MYH10*-2263: 5′-G AAUUGGACCCAAA CUUGUACAGAAAG-3′, 3′-UA CUUAACCUGGGU-UUGAACAUGUCUU-5′.
Quantitative PCR of *MYH9* mRNA was performed using primers 5′-CACTGAGACGGCCGATGC-3′ and 5′-GTC CCCGCGCCTGAG-3′, with probe 5′-ATGAACCGCG AAGTCAGCTCCCTAAAGAAC-3′; and for *MYH10*, primers 5′-CCTGCGAACCCTCCTGGT-3′ and 5′-TTT TATCTGTGGC TTTAGGGAACC-3′, with probe 5′-T ACTGGCCCTTTTGGATG-3′. Probes had a FAM fluorophore and a TAMRA quencher attached (Sigma-Genosys). Mitochondrial DNA copy number was estimated by comparing the abundance of the mitochondrial cytochrome *b* gene to that of the nuclear APP gene, as described (14). Twinkle siRNA was as previously described (14).

Confocal microscopy

HOS cells were washed and live-stained with 3 μl PicoGreen reagent (Invitrogen) and 100 nM of mitotracker orange (Invitrogen) as described (14,15). The excitation/emission wavelengths for PicoGreen and mitotracker orange were 502/523 nm and 554/576 nm, respectively. DNA, NM-IIB, and β-actin were labelled in fixed cells using a 1:200 mouse anti-DNA antibody (PROGEN Biotechnik), 1:50 anti-rabbit NM-IIB antibody and 1:3000 anti-β-actin (SIGMA). Secondary antibodies were 1:1000 anti-mouse Alexa Fluor 488 (Invitrogen) for DNA and β-actin, and 1:5000 anti-rabbit Alexa Fluor 488 (Invitrogen) for NM-IIB. A Radiance2000 (BIORAD) or a Zeiss LSM 510 confocal microscopy system was used for cell imaging. Images were acquired with a 60× or 63× oil immersion objective and processed in Adobe Photoshop. Nucleoid number and area were quantified using Andor iQ software.

DNA and protein analysis

MEF cells and mitochondria were lysed with extraction buffer (EB) containing 75 mM NaCl, 50 mM EDTA, 20 mM HEPES-NaOH (pH 7.8) and 0.5% SDS. The lysate was extracted successively with phenol and chloroform/isoamyl alcohol (24:1), and DNA resuspended in 20 mM HEPES pH 7.25. Three micrograms of total cellular DNA (three separate isolates for both cell types) was digested with *Blp*I, and the fragments resolved by agarose gel electrophoresis and visualized by Southern hybridization using radiolabelled probes directed against mouse mtDNA (nucleotides 14 866–15 331) and nuclear DNA (18S rDNA). Signal quantification relied on a Molecular Imager FX phosphorimager (Typhoon™, GE Healthcare).

Immunoprotein detection utilised antibodies to NM-IIA 1:2000 (Sigma), β-actin 1:15 000 (Sigma), the intermediate filament vimentin, or VIM 1:500 (Abcam), the microtubule protein β-tubulin (Sigma), the mitochondrial outer membrane protein TOM20 (Santa Cruz), the intermembrane space protein cytochrome *c*, or CYC 1:200, the inner mitochondrial membrane protein cytochrome *c* oxidase subunit II, or COX2 (Abcam), the mitochondrial chaperone HSP60 (Abcam), mitochondrial transcription factor A, or TFAm 1:40 000, ATPase family AAA domain-containing protein 3, or ATAD3 1:50 000, and cytosolic glyceraldehyde dehydrogenase, or GAPDH 1:5000 (Abcam). Secondary antibodies were anti-rabbit and anti-mouse HRP 1:1000 (Promega). These antibodies were used to probe membranes containing proteins separated on NuPAGE 4–12% SDS–PAGE (Invitrogen).

Sucrose-gradient purified mitochondria from HEK cells (2 mg/ml) were suspended in 20 mM HEPES pH 7.8, 2 mM EDTA, 210 mM mannitol, 70 mM sucrose and treated with or without 100 μg/ml of trypsin at room temperature for 30 min. After washing and pelleting mitochondria three times, the organelles were lysed with 0.4% DDM and centrifuged for 10 min at $1000g_{max}$; the supernatant was loaded on a 20–42.5% iodixanol gradient (20 mM HEPES pH 7.8, 1 mM EDTA, 50 mM NaCl, 2 mM DTT, 0.05% DDM with protease inhibitor) and centrifuged at $100\,000g_{max}$ for 14 h. Nucleic acid was extracted from a portion of each fraction of the gradient and after Southern blotting, hybridized to a radiolabelled probe to estimate the level of mtDNA, the remainder of each fraction was analysed by immunoblotting after SDS–PAGE.

RESULTS AND DISCUSSION

In a previous study, we isolated mitochondrial nucleoprotein complexes (nucleoids) from rat liver mitochondria using a generic DNA binding protein from *Escherichia coli*, HU (11). Here crude mitochondrial nucleoids were rigorously washed in a 900 mM NaCl solution to remove all but the most tightly associated proteins from the mtDNA. TFAM, for instance, dissociates from mtDNA under these conditions (Supplementary Figure S1A). Mass spectrometry repeatedly identified only six proteins in the final pellet that was highly enriched for mtDNA (Figure 1 and Table 1). Two mitochondrial proteins, ATAD3 and NIPSNAP1, were also present in our previous mitochondrial nucleoprotein preparations (Figure 1D) (11). The fact that ATAD3 and NIPSNAP1 co-purify with mtDNA using two different protocols strengthens their designation as nucleoid proteins. Another of the proteins present in the high-salt treated mtDNA preparations was prohibitin. Prohibitin is a well-established mitochondrial membrane protein with roles in protein processing, cristae formation and mitochondrial morphogenesis (16). Although prohibitin was not among the handful of proteins associated with HU-affinity purified mtDNA (11), it was present in mitochondrial nucleoprotein preparations of *Xenopus* oocytes and cultured human cells (10,17). Moreover, as with ATAD3 gene knockdown (11), prohibitin gene-silencing produces a marked decrease in PicoGreen staining of mitochondrial nucleoids (18). Prohibitin is important for mtDNA stability in yeasts and Langer and colleagues propose that the ring-like prohibitin complex can form a scaffold contributing to the integrity of the mitochondrial inner membrane (19). This would fit well with the idea of it stabilizing mtDNA, while permitting it to have other functions, such as its well-documented roles in protein processing (16). The presence of prohibitin in mtDNA-enriched material reported here adds to the growing body of evidence suggesting it contributes to mtDNA maintenance in mammals, as well as yeasts. Although uricase was the most abundant protein sedimenting with mitochondrial nucleoprotein (Figure 1C), it was almost certainly a contaminant, as it forms large crystals, which happen to sediment at the centrifugal forces used to harvest mitochondrial nucleoprotein complexes, and it is not expressed in humans (20).

Mitochondrial DNA and cytoskeletal factors

The remaining two candidate nucleoid proteins were β-actin and non-muscle myosin heavy chain IIA (NM-IIA), which form microfilaments that are a key component of the cytoskeleton. Immunoblotting of samples derived from rat liver mitochondria confirmed that, while only a small proportion of total cellular β-actin co-purifies with mitochondria (Figure 1E), mitochondrial-associated β-actin is enriched in $1000g_{max}$ supernatants together with mitochondrial DNA polymerase γ (Figure 1E), and mtDNA (Figure 1A). NM-IIA and its close relative NM-IIB are class II non-muscle myosin motor proteins, which are known to play important roles in diverse cellular functions including cytokinesis, morphogenesis and cell polarity (21). NM-IIA and NM-IIB share 77% identity at the amino acid level, and the ability of NM-IIA to complement some of the deficiencies associated with ablation of NM-IIB suggests considerable functional overlap between the two proteins (22). Inspection of the mass spectrometry data revealed that some masses were unique to NM-IIA, whereas no unique NM-IIB peptides were detected, suggesting that NM-IIB was absent from the rat liver mitochondrial nucleoprotein preparations. Of the two proteins, NM-IIA is relatively more abundant in rodent liver than several other tissues (23), and so the amount of NM-IIB in our preparations may have been below the limit of detection. Alternatively, NM-IIB may not bind as tightly to mitochondrial nucleoids as NM-IIA, and so may have dissociated during the high-salt isolation procedure ('Materials and Methods' section).

As a further test of the association of NM-IIA and β-actin with mtDNA, TFAM with a Streptactin tag was expressed in HEK.293T cells and the tagged protein recovered by affinity purification, after mitochondrial purification and lysis. Immunoblotting of NM-IIA, β-actin and SSBP1 in fractions sampled during the purification procedure indicated that all three proteins were captured together with mtDNA (Supplementary Figure S1B).

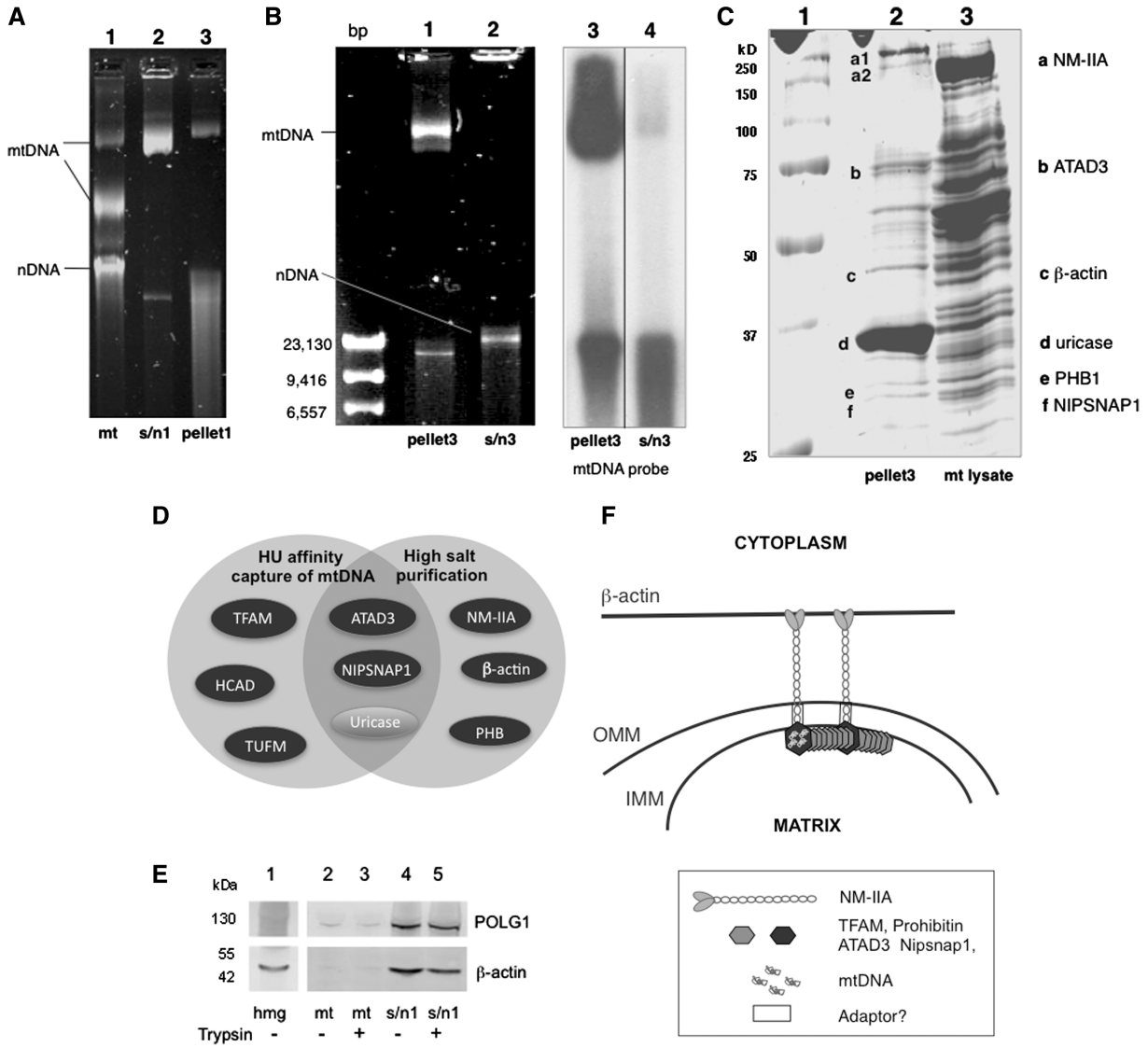

Figure 1. Enrichment of mitochondrial nucleoprotein via differential centrifugation and high-salt treatment. (**A**) DNA associated with sucrose-gradient purified rat liver mitochondria (mt) was analysed by agarose gel electrophoresis, before (lane 1) and after detergent lysis and $1000g_{max}$ centrifugation for 10 minutes (lanes 2 and 3). The first supernatant (s/n1) was centrifuged at $30\,000g_{max}$ for 30 min to sediment the bulk of the mtDNA and the pellet (2) was subjected to stringent washing in 900 mM NaCl, before being re-centrifuged ($30\,000g_{max}$, 60 min). (**B**) DNAs extracted from a fraction of pellet 3 and supernatant 3 were analysed by ethidium bromide staining (lanes 1 and 2) or by Southern hybridization to a probe corresponding to the large non-coding region of rat mtDNA (lanes 3 and 4, the two lanes shown were run on the same gel but in lanes that were not adjacent). (**C**) proteins separated by 12–22% SDS–PAGE and stained with Coomassie blue; lane 1—molecular mass markers; lane 2—proteins associated with the third pellet which contained the bulk of the intact mtDNA; lane 3—total mitochondrial lysate. Six proteins were identified by mass spectrometry with an error tolerance <70 ppm (Table 1); n = two independent experiments. (**D**) a Venn diagram showing the sets of candidate nucleoid proteins identified in this (high-salt purification) and an earlier study based on affinity capture of mtDNA with a generic DNA binding protein, HU (11), see main text for details. (**E**) immunoblotting of the first $1000g_{max}$ supernatant (s/n1), mitochondria (mt) and rat liver homogenate (hmg) with antibodies to POLG1 and β-actin. Trypsin treatments (+), which preceded lysis of mitochondria, were 50 μg/ml for 30 min at 37°C. (**F**) Preliminary model of the organization of mtDNA with candidate nucleoid proteins. OMM—outer mitochondrial membrane, IMM—inner mitochondrial membrane. NM-IIA—non-muscle myosin heavy chain IIA, ATAD3—ATPase family AAA domain-containing protein 3A, Nipsnap1: 4-nitrophenylphosphatase domain and non-neuronal SNAP25-like protein homologue 1.

Modulating *MYH9* and *MYH10* expression affects mtDNA copy number and topology

Transfection of human osteosarcoma (HOS) cells with siRNA capable of decreasing *MYH9* or *MYH10* expression to 10–15% of control values (Supplementary Figure S2A) produced two mtDNA-related phenotypes. There was a pronounced decrease in PicoGreen staining of mitochondrial nucleoids after *MYH9* or *MYH10* siRNA treatment (Figure 2A and Supplementary Figure S2B). PicoGreen staining of DNA depends largely on the arrangement of DNA: supercoiled DNA produces a lower signal per unit mass of DNA than relaxed circles. Previously we documented a marked decrease in PicoGreen staining associated with a modest decrease in mtDNA copy number, after ATAD3 siRNA

Table 1. Proteins co-purifying with rat liver mtDNA after differential centrifugation of mitochondrial lysates and high salt treatment, identified by MALDI-peptide mass fingerprinting

Band	Protein	Accession no.	Molecular Mass (kDa)		MALDI-TOF MS Data[a]		
		NCBI gi accession No.	Observed[b]	Predicted	Peptide matches[c]	Sequence coverage %	Mascot Score[d]
a1	NM-IIA[e]	6981236	234.9	226	23/30	16	150/76
a2			193.5	226	6/9	4	40/58
b	ATAD3A[f]	77415397	59.1	66	9/17	22	86/78
c	β-actin	71620	48.3	41	10/12	35	151/58
d	Uricase	20127395	34.9	34	12/23	37	131/76
e	Prohibitin	62664759	33.8	29	8/27	42	86/58
f	Nipsnap1[g]	34879019	30.5	33	7/19	23	59/76[h]

Data are for tryptic peptides. Number of entries of NCBInr database: 3023944.
[a]Derived from proteins enriched from 3–6 mg lots of mitochondria.
[b]Observed masses in kiloDaltons (kDa) were based on protein standards. The equation used was $y = 0.133x^4 - 3.8757x^3 + 39.963x^2 - 176.58x + 333.81$, $R^2 = 0.976$.
[c]number of mass matches/total masses searched.
[d]mass tolerance parameter used: 70 ppm.
[e]NM-IIA: Non-muscle myosin heavy chain IIA; NMMHC II-a; NMMHC-IIA; MYH9, Myosin non-muscle heavy chain 9; Myosin heavy chain, non-muscle IIA; Cellular myosin heavy chain, type A.
[f]ATAD3: ATPase family AAA domain-containing protein 3A (ATAD3A) in rat; ATPase family AAA domain-containing protein 3B (ATAD3B) in human; AAA-ATPase TOB3; TOB3.
[g]Nipsnap1: 4-nitrophenylphosphatase domain and non-neuronal SNAP25-like protein homologue 1.
[h]four peptides analysed by tandem MS matched Nipsnap1.

treatment (11). In the case of *MYH9* or *MYH10* gene-silencing, the *decrease* in PicoGreen staining of mitochondrial nucleoids was accompanied by a 1.5-fold *increase* in mtDNA copy number, based on quantitative (Q-) PCR (Figure 2B). Moreover, the increase in copy number reached 3.3 times that of controls when siRNAs targeting *MYH9 and MYH10* were employed together (Figure 2B). Thus, NM-IIA and NM-IIB each contribute to mtDNA homeostasis.

Mitochondrial DNA depletion in mouse embryonic fibroblasts lacking NM-IIB

MYH10 has been ablated in mice (24), enabling us to determine the contribution of NM-IIB to mtDNA maintenance. Based on Southern hybridization mtDNA copy number was reduced to 38% of control values in $MYH10^{-/-}$ mouse embryonic fibroblasts (Figure 3A). Q-PCR also indicated a substantial decrease in mtDNA copy number in cells lacking NM-IIB (Supplementary Figure S2C), whereas the abundance of an outer and an inner mitochondrial membrane protein were unaffected by the loss of *MYH10* (Supplementary Figure S3A), suggesting there was no generalized decrease in mitochondria in $MYH10^{-/-}$ cells. Therefore, loss of *MYH10* causes mtDNA depletion.

The absence of NM-IIB was associated with changes in mitochondrial morphology, as well as mtDNA depletion: confocal microscopy revealed extensive fragmentation of the mitochondrial network in many more $MYH10^{-/-}$ cells, than control cells (Figure 3B, 3C-v and 3C-xi). There was also a significant increase in the number of cells in which mitochondria were not as widely distributed as in control cells, but had a more central location close to the nucleus; these were designated as having 'contracted' mitochondria (3C-vi and 3C-xii) (see also β-actin siRNA below). Comparison of $MYH10^{+/+}$ and $MYH10^{-/-}$ MEFs revealed no significant difference in the number ($P = 0.51$) or size ($P = 0.91$) of nucleoids in cells with normal mitochondrial morphology. $MYH10^{-/-}$ cells with 'contracted' mitochondria had fewer nucleoids, whereas those cells with a fragmented mitochondrial network had smaller nucleoids, yet similar numbers of nucleoids to control cells (Figure 3D). Hence, mitochondrial fragmentation in $MYH10^{-/-}$ cells was associated with a reduction in the number of copies of mtDNA per nucleoid. None of these changes had an appreciable effect on the growth rate of the MEFs (Supplementary Figure S3B).

The opposite effects of a shortage of NM-IIB on mtDNA copy number of HOS cells (Figure 2B) and MEFs (Figure 3A) might reflect differences in mitochondrial nucleoid composition between the two cell types. The ability of MEFs to tolerate the loss of *MYH10* implies reprogramming of gene expression to adapt to the loss of the gene. Monitoring mtDNA in a conditional knockout mouse could clarify whether or not an increase in mtDNA level is the typical initial response to a shortage of NM-IIB (or NM-IIA).

β-actin siRNA perturbs mtDNA mass, organization and mitochondrial morphology

β-actin siRNA produced a 40% decrease in mtDNA copy number, 48–96 h after transfection of HOS cells, based on Q-PCR analysis (Figure 4A). Thereafter copy number rose and 144 h after transfection mtDNA copy number exceeded the level of control cells (Figure 4A), despite the fact that β-actin expression remained low (Figure 4B, Supplementary Figure S4A). β-actin siRNA was also associated with contraction of mitochondria away from the cell periphery, and with mitochondrial fragmentation (Figure 4B and C). Fragmentation of the

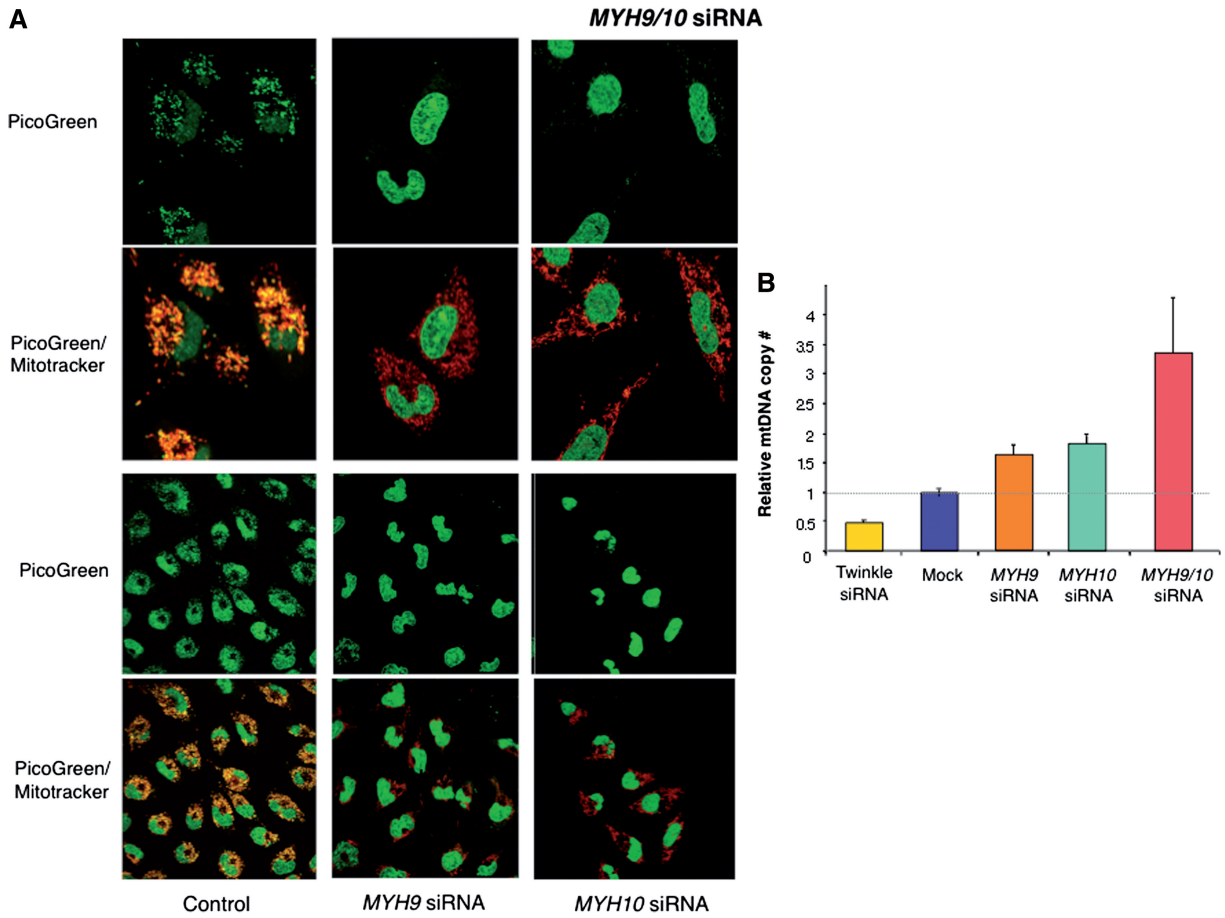

Figure 2. MHY9 siRNA affects mtDNA topology and copy number. (**A**) HOS cells transfected twice with dsRNA *MYH9*-2806 or *MYH10*-2783 were stained with PicoGreen (green) and mitotracker (red) and examined by confocal microscopy at 1200× and 600× magnification; $t = 144$ h. (**B**) MtDNA copy number was estimated via Q-PCR of HOS cell DNA after 144 h of *MYH9* and/or *MYH10* siRNA. Because initial results suggested an increase in mtDNA copy number, Twinkle siRNA was carried out in parallel for 72 h, as this was known to cause mtDNA depletion (14). $n = 4$ experiments for *MYH9* and *MYH10 siRNA* and $n = 2$ for Twinkle. Errors are ±1 standard deviation from the mean.

mitochondria increased with the duration of gene silencing, whereas contracted mitochondria were most prevalent 48 h after transfection, and declined in number thereafter (Figure 4C and Supplementary Figure S4B). Those cells defined as having contracted mitochondria had larger and fewer nucleoids than controls ($P < 0.001$) (Figure 4D), while nucleoids were also fewer in number in cells with fragmented mitochondria, the difference was less marked (Figure 4D). Thus, the fragmentation of mitochondria may relieve the constraint on mtDNA replication imposed by the paucity of β-actin, and thereby explain the increase in mtDNA copy number observed between the 96 and 144 h time points (Figure 4A). The increase in mtDNA copy number between 96 and 144 h of β-actin siRNA was substantial (2-fold) and highly significant ($P < 0.001$). Although there was a modest increase in β-actin 144 h after the first siRNA transfection compared to earlier time points, the level of the protein remained well below that of control cells (Figure 4B-iii, Supplementary Figure S4A) and so the level of β-actin was not directly proportional to the number of mtDNA molecules per cell.

A fraction of β-actin and NM-IIA is located inside human mitochondria

The majority of β-actin and NM-IIA reside in the cytoplasm outside mitochondria, and so the initial presumption was that β-actin and NM-IIA were linked to mtDNA via adaptor proteins that bridge the mitochondrial membranes (Figure 1F). Mitochondrial nucleoprotein complexes can be resolved on iodixanol gradients, and analysed by Southern and immunoblotting, after organelle lysis (25). Here this approach, applied to HEK cell derived mitochondria, demonstrated that some β-actin and NM-IIA co-fractionate with mtDNA and TFAM, whereas the majority of mitochondrial proteins resolve near the top of the gradient, e.g. COX2 and HSP60 (Figure 5A-i and Supplementary Figure S5). A substantial amount of the β-actin and NM-IIA associated with human mitochondria survived when isolated mitochondria were treated with trypsin, prior to lysis and iodixanol gradient fractionation (Figure 5A-ii). In contrast, the mitochondrial outer membrane protein TOM20 and the cytoskeletal proteins β-tubulin and vimentin were completely degraded by trypsin

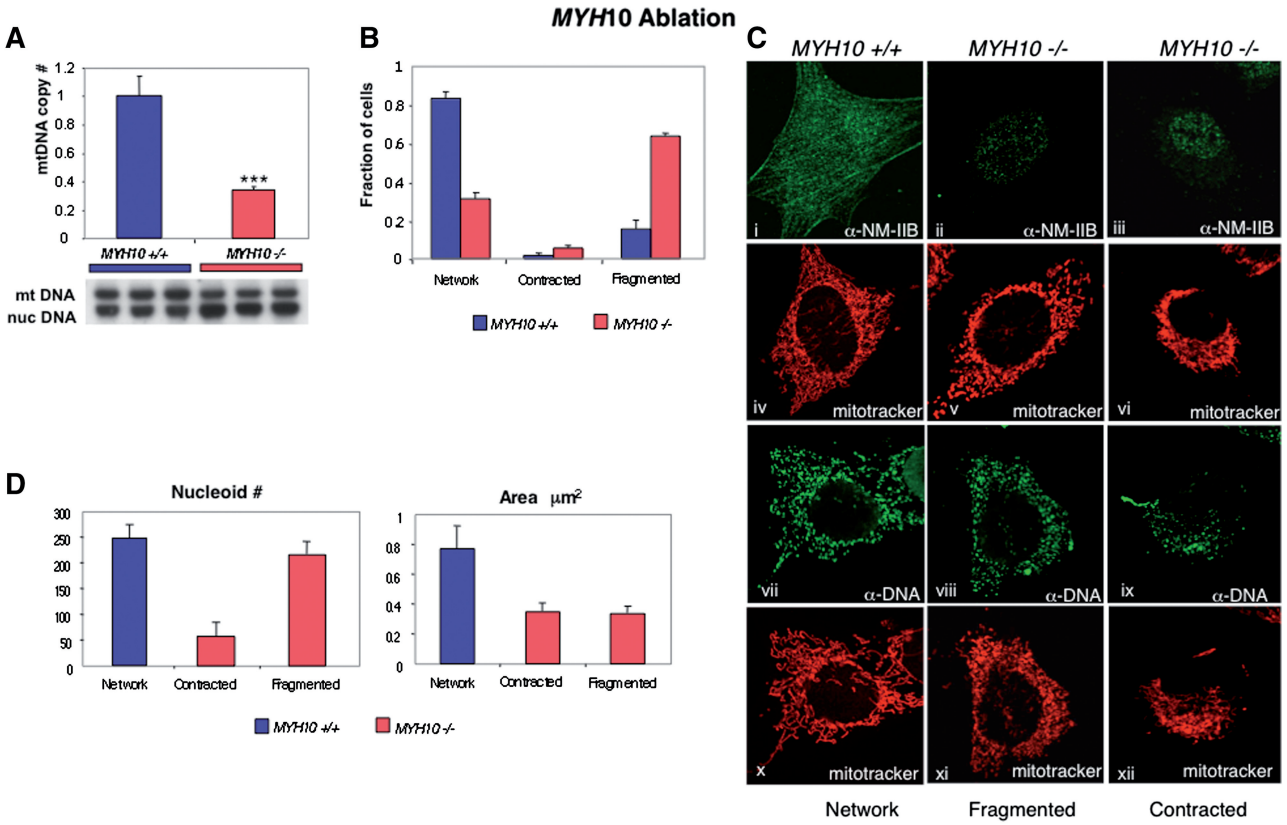

Figure 3. Loss of *MYH10* is associated with mtDNA depletion and changes in mtDNA organization and mitochondrial morphology in mouse embryonic fibroblasts. (**A**) DNA was harvested from control ($MYH10^{+/+}$) and $MYH10^{-/-}$ MEFs and mtDNA copy number estimated by Southern blotting with probes specific for mtDNA and nuclear DNA ($n = 3$ independent experiments). (**B**) the distribution of mitochondria was classified as one of three types based on visual inspection; the mitochondria of most control cells ($NM\text{-}IIB^{+}/B^{+}$) formed an extensive 'network' extending to the cell's periphery; however in some cells the mitochondria were concentrated close to the nucleus (contracted), in still other cells the mitochondria were widely distributed but discontinuous, or fragmented. Approximately 80 $MYH10^{+/+}$ cells and 80 $MYH10^{-/-}$ cells were screened and assigned to one of the three categories. (**C**) MEF *MYH10* +/+ and $MYH10^{-/-}$ cells labelled with anti-NM-IIB, the mitochondrial specific stain, mitotracker or anti-DNA antibody. The antibody to NM-IIB weakly cross-reacted with a nuclear protein, which was only visible when NM-IIB was absent. (**D**) Nucleoid number and area were determined in 10 cells per mitochondrial phenotype.

(Figure 5A-ii). Furthermore, the surviving β-actin and NM-IIA was concentrated in the same fractions of the iodixanol gradients as the mtDNA, corroborating the initial finding that both these proteins are associated with mtDNA (Figure 1 and Supplementary Figure S1B). ATAD3 also co-fractionated with TFAM and mtDNA (Figure 5A).

Next human β-actin and the closely related β-actin-like 2 were synthesised *in vitro* using reticulocyte lysates and incubated with isolated rat liver mitochondria. A small amount (6%) of β-actin, but not its close relative β-actin-like 2, survived trypsin treatment after incubation with mitochondria, implying that it was imported into mitochondria (Figure 5B). Dissipating the membrane potential with the chemical uncoupler FCCP blocks energy-dependent import of mitochondrial proteins, and the addition of FCCP reduced the amount of β-actin surviving trypsin treatment to <1% of the total (Figure 5B), as was the case for TFAM (data not shown). Thus, the uptake of β-actin by isolated mitochondria is largely dependent on the mitochondria maintaining an electrochemical gradient across the IMM. Although actin is best known for its cytoskeletal functions in the cytoplasm it also contributes to several essential processes in the cell nucleus, including chromatin remodelling and transcription (26). Nuclear actin works in conjunction with actin-binding proteins, rather than binding to DNA directly, and so we envisage a similar situation in mitochondria.

Co-enrichment of β-actin and NM-IIA with rat liver mtDNA (Figure 1), and co-fractionation of the same two proteins with human mtDNA, after protease-digestion of extra-mitochondrial protein (Figure 5A), combined with the membrane-potential dependent import of β-actin into isolated mitochondria (Figure 5B) suggests that a fraction of these proteins is located inside mitochondria, associated with mtDNA, where they may well form a microfilament. Bacteria were long believed to lack a cytoskeleton, yet there is now concrete evidence they possess structural and functional homologues of the eukaryotic cytoskeletal proteins actin and tubulin (27). Given the mitochondrion's prokaryotic origins, it is highly plausible that they too have a superstructure or 'mitoskeleton', to support the mitochondrial nucleoid,

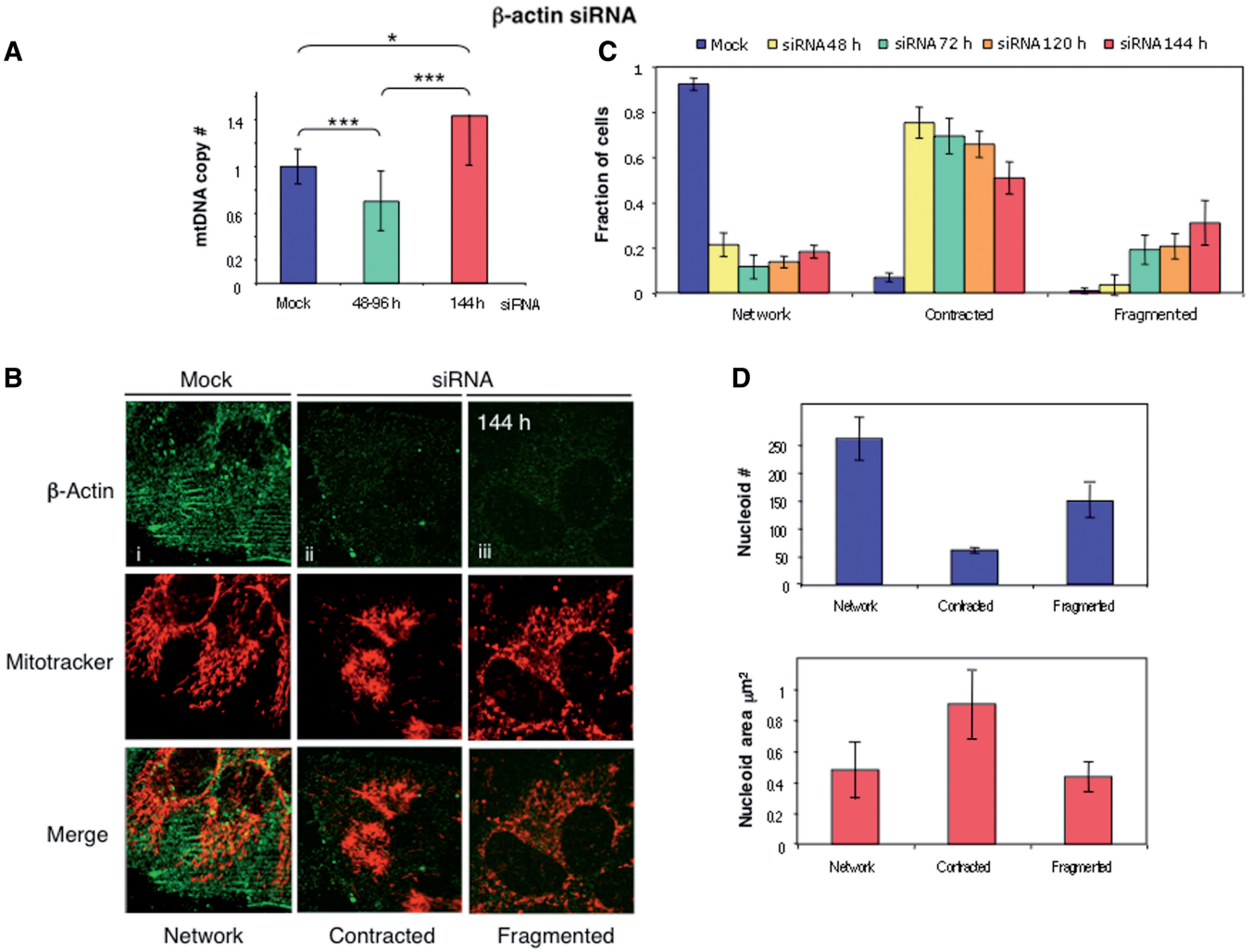

Figure 4. β-Actin siRNA perturbs mtDNA mass, organization and mitochondrial morphology. (**A**) HOS cell DNA was analysed by Q-PCR at intervals after transfection of cells with an siRNA targeting β-actin. A 40% decrease in mtDNA copy number was observed 48 72 and 96 h after transfection, which was statistically significant only at the 96 h time point ($P = 0.0087$); however, when results for the three time points were combined, the consistent decrease in mtDNA copy number was highly significant ($^{***}P < 0.001$). Mitochondrial DNA copy number was highest 144 h after transfection; the difference from mock transfected cells just achieved significance ($^{*}P < 0.05$), whereas it was more marked compared to the 96 h time point ($^{***}P < 0.001$). (**B**) immunocytochemistry with an antibody to β-actin indicated that siRNA was effective at repressing β-actin expression for up to 144 h, and this was associated with 'contraction' of mitochondria away from the peripheral parts of the cell, and with mitochondrial fragmentation. (**C**) after mock transfection or β-actin RNAi, a minimum of 80 cells were scored as having normal (network), contracted or fragmented mitochondria, at each time point. (**D**) the number and size (area) of mitochondrial nucleoids were determined in 10 cells for each mitochondrial phenotype. The network phenotypes were obtained from mock-transfected cells, whereas cells with contracted or fragmented mitochondria were from cells subjected to β-actin RNAi.

among other things. Notwithstanding this, the proposed intra-mitochondrial actomyosin association with mitochondrial nucleoids (Figure 6) does not exclude a role for cytoplasmic actomyosin in mtDNA maintenance.

Based on the results reported here, perturbation of both β-actin and *MYH9/10* expression can cause mtDNA copy to increase or decrease, dependent on the duration and extent of the perturbation (Figures 3 and 4, Supplementary Figures S2 and S4). Thus, we conclude the proteins have an organizational and structural role in mtDNA maintenance and are not themselves regulating mtDNA copy number. Temporal studies of the expression of other mitochondrial nucleoid proteins, in response to β-actin or *MYH9/10* siRNA could help to clarify how cells adapt to a dearth of these proteins, and thereby explain the fluctuations in mtDNA copy number. The changes in mitochondrial nucleoids and mitochondrial morphology that accompany decreased expression of *MYH9* and β-actin genes, and ablation of *MYH10* (Figures 2–4), coupled with the physical association of the NM-IIA and β-actin proteins with mtDNA (Figures 1 and 5) are all consistent with the hypothesis that actomyosin filaments offer structural support to the mitochondrial network and mtDNA in mammalian cells. Perturbation of the cytoskeleton could indirectly affect mtDNA, in the same way that disruption or mutation of various proteins required for normal mitochondrial morphology and movement can affect mtDNA stability, e.g. (28), and

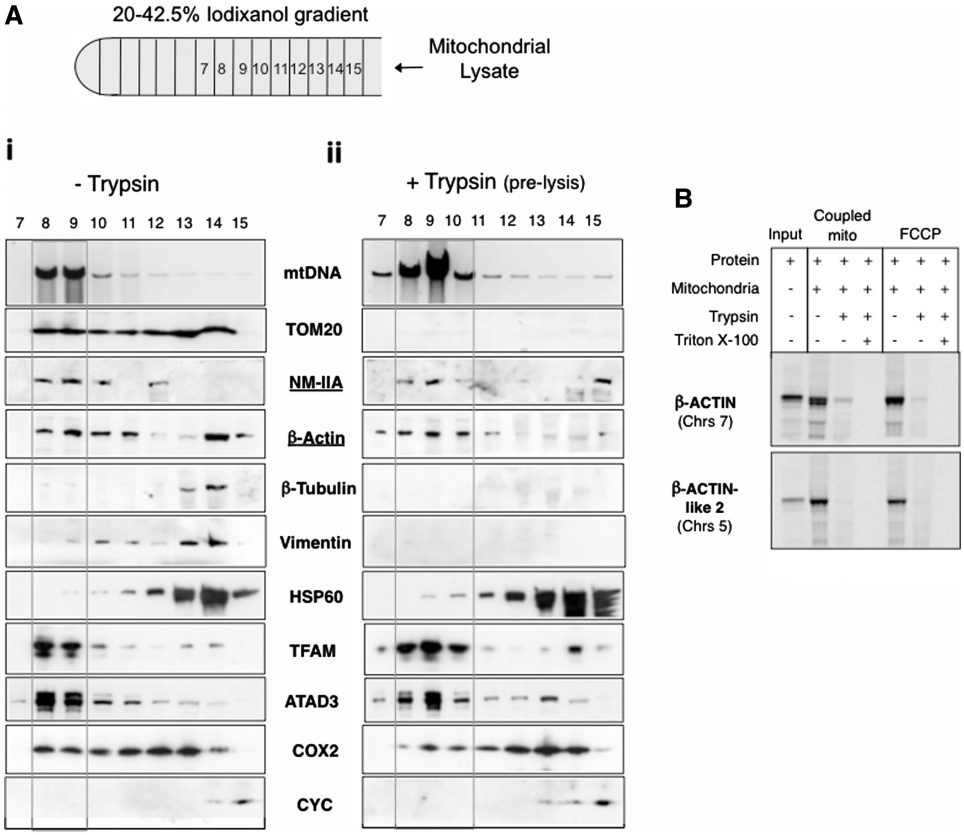

Figure 5. A protease-resistant population of β-actin and NM-IIA co-fractionates with human mitochondrial DNA. (**A**) Mitochondria isolated from HEK cells by differential and sucrose gradient centrifugation were treated without (−) or with (+) trypsin, prior to lysis and fractionation on an iodixanol gradient. Protein and DNA were recovered from the different fractions (15 in total) and analysed by immuno or Southern blotting. (Fractions 1–6 were blank in all cases and do not appear as part of the figure.) The DNA probe was specific for human mtDNA, whereas the antibodies applied were designed to detect the outer mitochondrial membrane protein TOM20, the cytoskeletal proteins β-actin, NM-IIA, β-tubullin and vimentin, the mitochondrial matrix chaperone HSP60, the mtDNA binding protein TFAM, the candidate nucleoid protein ATAD3, an inner mitochondrial membrane protein COX2 and CYC, which is located between the outer and inner mitochondrial membranes in the intermembrane space. (Another IMS protein AK2 showed an identical distribution to CYC, data not shown.) Boxes demarcate the fractions where the mtDNA was concentrated. The amount of protein present in the iodixanol gradient fractions containing mtDNA (8–10), where β-actin survived trypsin treatment, was lower than other fractions (14 and 15), where it did not, (Supplementary Figure S4); and none of the protein recovered from iodixanol gradients was inherently trypsin-resistant (Supplementary Figure S5). (**B**) β-actin, but not β-actin-like 2 is imported into mitochondria. *In vitro* synthesised human β-actin and β-actin-like 2, before and after incubation with isolated rat liver mitochondria, separated by 12% SDS–PAGE ('Materials and Methods').

so the challenge for the future will be to elucidate the respective contributions of intra- and extra-mitochondrial β-actin and NM-IIA/B to mtDNA maintenance. This will be all the more difficult as mitochondrial import of β-actin appears to be stochastic (Figure 5B), and not dependent on a dedicated mitochondrial form of the protein.

Given the well-recognized role of myosin family proteins in movement, NM-IIA and IIB are strong candidates for playing a key role in mtDNA segregation or transmission. Other nucleoid proteins such as ATAD3, may also form part of the mtDNA segregation apparatus (29) as well as contributing to mtDNA packaging (Figure 6).

NM-IIA/B and human disease

Pathological mutations in *MYH9* cause hearing loss, kidney dysfunction and haemopoietic disorders in humans (30), clinical features that are common to many mitochondrial disorders (31). In light of this report, impaired mtDNA homeostasis may account for one or more of the clinical features associated with known, or as yet to be described, mutations in *MYH9*. In particular, a mitochondrial (DNA) contribution to hearing impairment should be considered because much of the NM-IIA of cochlear hair cells is located in the mitochondrial inner membrane, based on immuno-gold electron microscopy (32).

SUPPLEMENTARY DATA

Supplementary Data are available at NAR Online.

ACKNOWLEDGEMENTS

TFAM antibody and antibodies to CYC and AK2 were kind gifts of Drs R. Weisner and M. Murphy, respectively.

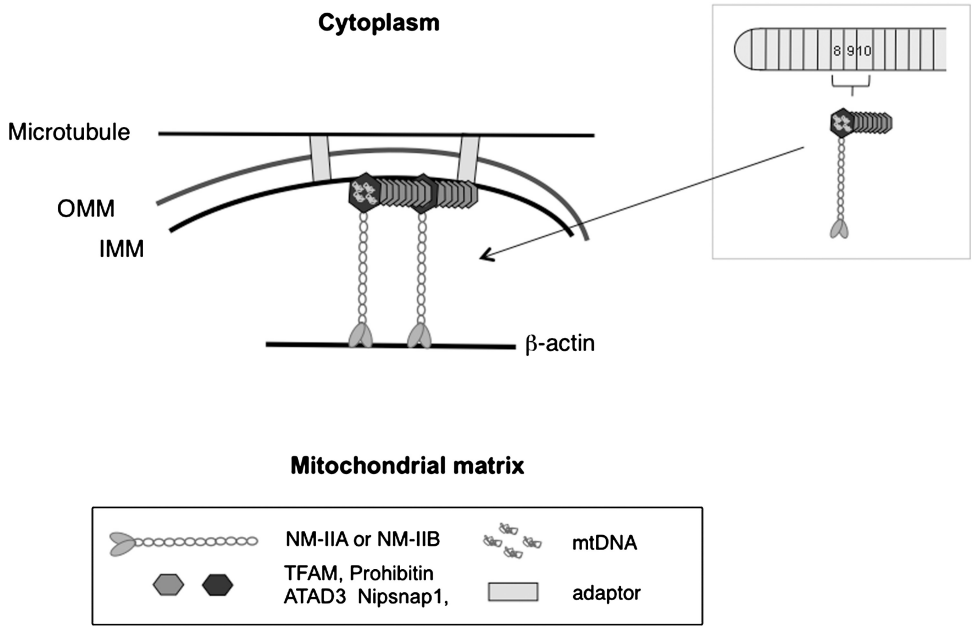

Figure 6. Possible arrangement of intra-mitochondrial actomyosin in relation to mtDNA and nucleoid proteins. The most abundant proteins in enriched rat mtDNA preparations identified in this report (Figure 1C) and an earlier study (11) were TFAM, ATAD3, NIPSNAP1, NM-IIA, β-actin, TUFM and Prohibitin. Furthermore, TFAM, ATAD3, NM-IIA and β-actin co-fractionate with mitochondrial nucleoprotein complexes resolved on iodixanol gradients (Figure 5A and inset). Given the known cytoskeletal properties of NM-IIA and β-actin, they are more likely to provide structural support to, and facilitate movement of mitochondrial nucleoids, than function as DNA packaging proteins (dark grey hexagons). Although a substantial majority of ATAD3 co-fractionates with mtDNA (Figure 5A), ATAD3 is more widely distributed in the mitochondrial network than mtDNA (11), and so many molecules of ATAD3 must be linked indirectly to mtDNA, presumably via protein–protein interactions (light grey hexagons). The depiction of nucleoprotein complexes bound to the mitochondrial inner membrane is based on the earlier demonstration of a tight association between mitochondrial membranes and ATAD3 and mtDNA (11). This model does not exclude that in Figure 1F, as cytoskeletal NM-IIA and β-actin may also contribute to mtDNA stability. Nor does the model obviate the need for other proteins, such as mitofilin, to provide structural support to mitochondria. OMM—outer mitochondrial membrane; IMM—inner mitochondrial membrane; NM-IIA—non-muscle myosin heavy chain IIA.

FUNDING

Medical Research Council; the European Union; the Intramural Research Program of the Eunice Kennedy Shriver National Institute of Child Health and Human Development and National Heart; Lung and Blood Institute; National Institutes of Health and grants [CMRPG360491-2, 380651, NSC 97-2321-B-182A-002-MY2] from the Chang Gung Memorial Hospital, Lin-Kou, Taiwan (to C.C.M.). Funding for open access charge: Medical Research Council.

Conflict of interest statement. None declared.

REFERENCES

1. Boldogh,I.R., Nowakowski,D.W., Yang,H.C., Chung,H., Karmon,S., Royes,P. and Pon,L.A. (2003) A protein complex containing Mdm10p, Mdm12p, and Mmm1p links mitochondrial membranes and DNA to the cytoskeleton-based segregation machinery. *Mol. Biol. Cell*, **14**, 4618–4627.
2. Hobbs,A.E., Srinivasan,M., McCaffery,J.M. and Jensen,R.E. (2001) Mmm1p, a mitochondrial outer membrane protein, is connected to mitochondrial DNA (mtDNA) nucleoids and required for mtDNA stability. *J. Cell. Biol.*, **152**, 401–410.
3. Meeusen,S. and Nunnari,J. (2003) Evidence for a two membrane-spanning autonomous mitochondrial DNA replisome. *J. Cell. Biol.*, **163**, 503–510.
4. Hollenbeck,P.J. and Saxton,W.M. (2005) The axonal transport of mitochondria. *J. Cell. Sci.*, **118**, 5411–5419.
5. Quintero,O.A., DiVito,M.M., Adikes,R.C., Kortan,M.B., Case,L.B., Lier,A.J., Panaretos,N.S., Slater,S.Q., Rengarajan,M., Feliu,M. *et al.* (2009) Human Myo19 is a novel myosin that associates with mitochondria. *Curr. Biol.*, **19**, 2008–2013.
6. Boldogh,I.R. and Pon,L.A. (2006) Interactions of mitochondria with the actin cytoskeleton. *Biochim. Biophys. Acta*, **1763**, 450–462.
7. Iborra,F.J., Kimura,H. and Cook,P.R. (2004) The functional organization of mitochondrial genomes in human cells. *BMC Biol.*, **2**, 9.
8. Kanki,T., Nakayama,H., Sasaki,N., Takio,K., Alam,T.I., Hamasaki,N. and Kang,D. (2004) Mitochondrial nucleoid and transcription factor A. *Ann. NY Acad. Sci.*, **1011**, 61–68.
9. Pellegrini,M., Asin-Cayuela,J., Erdjument-Bromage,H., Tempst,P., Larsson,N.G. and Gustafsson,C.M. (2009) MTERF2 is a nucleoid component in mammalian mitochondria. *Biochim. Biophys. Acta*, **1787**, 296–302.
10. Wang,Y. and Bogenhagen,D.F. (2006) Human MTDNA nucleoids are linked to protein folding machinery and metabolic enzymes at the mitochondrial inner membrane. *J. Biol. Chem.*, **281**, 25791–25802.
11. He,J., Mao,C.C., Reyes,A., Sembongi,H., Di Re,M., Granycome,C., Clippingdale,A.B., Fearnley,I.M., Harbour,M., Robinson,A.J. *et al.* (2007) The AAA+ protein ATAD3 has displacement loop binding properties and is involved in mitochondrial nucleoid organization. *J. Cell. Biol.*, **176**, 141–146.
12. Yang,M.Y., Bowmaker,M., Reyes,A., Vergani,L., Angeli,P., Gringeri,E., Jacobs,H.T. and Holt,I.J. (2002) Biased incorporation of ribonucleotides on the mitochondrial L-strand accounts for apparent strand-asymmetric DNA replication. *Cell*, **111**, 495–505.

13. Petruzzella,V., Tiranti,V., Fernandez,P., Ianna,P., Carrozzo,R. and Zeviani,M. (1998) Identification and characterization of human cDNAs specific to BCS1, PET112, SCO1, COX15, and COX11, five genes involved in the formation and function of the mitochondrial respiratory chain. *Genomics*, **54**, 494–504.
14. Tyynismaa,H., Sembongi,H., Bokori-Brown,M., Granycome,C., Ashley,N., Poulton,J., Jalanko,A., Spelbrink,J.N., Holt,I.J. and Suomalainen,A. (2004) Twinkle helicase is essential for mtDNA maintenance and regulates mtDNA copy number. *Hum. Mol. Genet.*, **13**, 3219–3227.
15. Ashley,N., Harris,D. and Poulton,J. (2005) Detection of mitochondrial DNA depletion in living human cells using PicoGreen staining. *Exp. Cell. Res.*, **303**, 432–446.
16. Merkwirth,C. and Langer,T. (2009) Prohibitin function within mitochondria: essential roles for cell proliferation and cristae morphogenesis. *Biochim. Biophys. Acta*, **1793**, 27–32.
17. Bogenhagen,D.F., Wang,Y., Shen,E.L. and Kobayashi,R. (2003) Protein components of mitochondrial DNA nucleoids in higher eukaryotes. *Mol. Cell. Proteomics*, **2**, 1205–1216.
18. Kasashima,K., Sumitani,M., Satoh,M. and Endo,H. (2008) Human prohibitin 1 maintains the organization and stability of the mitochondrial nucleoids. *Exp. Cell. Res.*, **314**, 988–996.
19. Osman,C., Haag,M., Potting,C., Rodenfels,J., Dip,P.V., Wieland,F.T., Brugger,B., Westermann,B. and Langer,T. (2009) The genetic interactome of prohibitins: coordinated control of cardiolipin and phosphatidylethanolamine by conserved regulators in mitochondria. *J. Cell. Biol.*, **184**, 583–596.
20. Volkl,A., Baumgart,E. and Fahimi,H.D. (1988) Localization of urate oxidase in the crystalline cores of rat liver peroxisomes by immunocytochemistry and immunoblotting. *J. Histochem. Cytochem.*, **36**, 329–336.
21. Conti,M.A. and Adelstein,R.S. (2008) Nonmuscle myosin II moves in new directions. *J. Cell. Sci.*, **121**, 11–18.
22. Bao,J., Ma,X., Liu,C. and Adelstein,R.S. (2007) Replacement of nonmuscle myosin II-B with II-A rescues brain but not cardiac defects in mice. *J. Biol. Chem.*, **282**, 22102–22111.
23. Golomb,E., Ma,X., Jana,S.S., Preston,Y.A., Kawamoto,S., Shoham,N.G., Goldin,E., Conti,M.A., Sellers,J.R. and Adelstein,R.S. (2004) Identification and characterization of nonmuscle myosin II-C, a new member of the myosin II family. *J. Biol. Chem.*, **279**, 2800–2808.
24. Tullio,A.N., Accili,D., Ferrans,V.J., Yu,Z.X., Takeda,K., Grinberg,A., Westphal,H., Preston,Y.A. and Adelstein,R.S. (1997) Nonmuscle myosin II-B is required for normal development of the mouse heart. *Proc. Natl Acad. Sci. USA*, **94**, 12407–12412.
25. Di Re,M., Sembongi,H., He,J., Reyes,A., Yasukawa,T., Martinsson,P., Bailey,L.J., Goffart,S., Boyd-Kirkup,J.D., Wong,T.S. *et al.* (2009) The accessory subunit of mitochondrial DNA polymerase gamma determines the DNA content of mitochondrial nucleoids in human cultured cells. *Nucleic Acids Res.*, **37**, 5701–5713.
26. Visa,N. and Percipalle,P. (2010) Nuclear functions of actin. *Cold Spring Harb. Perspect. Biol.*, **2**, a000620.
27. Errington,J. (2003) Dynamic proteins and a cytoskeleton in bacteria. *Nat. Cell Biol.*, **5**, 175–178.
28. Chen,X.J. and Butow,R.A. (2005) The organization and inheritance of the mitochondrial genome. *Nat. Rev. Genet.*, **6**, 815–825.
29. Holt,I.J., He,J., Mao,C.C., Boyd-Kirkup,J.D., Martinsson,P., Sembongi,H., Reyes,A. and Spelbrink,J.N. (2007) Mammalian mitochondrial nucleoids: organizing an independently minded genome. *Mitochondrion*, **7**, 311–321.
30. Heath,K.E., Campos-Barros,A., Toren,A., Rozenfeld-Granot,G., Carlsson,L.E., Savige,J., Denison,J.C., Gregory,M.C., White,J.G., Barker,D.F. *et al.* (2001) Nonmuscle myosin heavy chain IIA mutations define a spectrum of autosomal dominant macrothrombocytopenias: May-Hegglin anomaly and Fechtner, Sebastian, Epstein, and Alport-like syndromes. *Am. J. Hum. Genet.*, **69**, 1033–1045.
31. Finsterer,J. (2007) Hematological manifestations of primary mitochondrial disorders. *Acta Haematol.*, **118**, 88–98.
32. Lalwani,A.K., Atkin,G., Li,Y., Lee,J.Y., Hillman,D.E. and Mhatre,A.N. (2008) Localization in stereocilia, plasma membrane, and mitochondria suggests diverse roles for NMHC-IIa within cochlear hair cells. *Brain Res.*, **1197**, 13–22.